

# Two-dimensional array of diffusive SNS junctions with high-transparent interfaces

T. I. Baturina, Z. D. Kvon, and A. E. Plotnikov

*Institute of Semiconductor Physics, 630090, Novosibirsk, Russia*

We report the first comparative study of the properties of two-dimensional arrays and single superconducting film–normal wire–superconducting film (SNS) junctions. The NS interfaces of our SNS junctions are really high transparent, for superconducting and normal metal parts are made from the same material (superconducting polycrystalline PtSi film). We have found that the two-dimensional arrays reveal some novel features: (i) the significant narrowing of the zero bias anomaly (ZBA) in comparison with single SNS junctions, (ii) the appearance of subharmonic energy gap structure (SGS), with up to  $n = 16$  ( $eV = \pm 2\Delta/n$ ), with some numbers being lost, (iii) the transition from 2D logarithmic weak localization behavior to metallic one.

73.23.-b, 74.80.Fp, 74.50.+r, 73.20.Fz

Improvements in fabrication technology enable a variety of nanoscale mesoscopic hybrid structures to be made and phase-coherent transport to be studied. In the past few years, the mesoscopic systems, consisting of a normal metal (N) or heavily doped semiconductor being in contact with a superconductor (S), have been attracting an increasing interest mainly because of the richness of involved quantum effects [1]. The key mechanism governing the carrier transport through the NS contact is the Andreev reflection. In this process, an electron-like excitation with an energy  $\epsilon$  smaller than the superconducting gap  $\Delta$  moving from the normal metal to the NS interface is retro-reflected as a hole-like excitation, while Cooper pair is transmitted into the superconductor. This phenomenon is the basis of the proximity effect, which generally implies the influence of a superconductor on the properties of a normal metal being in electrical contact. Nowadays the comprehensive proximity effect is considered to be determined by the parameters of the normal part of the junction and by the properties of the NS interface in common. SNS systems may be classified with respect to the relation between the mean-free path and any other characteristic length in the system (either diffusive or ballistic regime) and by the transparency of the NS interfaces. At present, a large variety of NS and SNS junctions (most of them are diffusive) is fabricated and studied [2–13]. The investigations of these junctions are primarily focused on the nonlinear behavior of current-voltage characteristics which exhibit the zero bias anomaly (ZBA), the subharmonic energy gap structure (SGS), etc. Although much work has been done on single SNS junctions, it is an experimental challenge to fabricate and carry out comparative measurements on multiply connected SNS systems. In this Letter, we present the results of low-temperature transport measurements on two-dimensional arrays of SNS junctions (2DSNS) and on single SNS junctions and perform the comparative analysis of their properties.

The design of our samples is based on the fabrication technique of SNS junctions with perfect NS interfaces that was recently proposed and realized by us [13]. The

point is the losing superconductivity in the submicron constrictions made in the ultrathin polycrystalline PtSi superconducting film by means of electron beam lithography and subsequent plasma etching. The reason of that is not completely understood. Nevertheless, this processing allows us to obtain the SNS junctions, in which the superconducting and the normal metal parts are made from the same material. In that way we escape from unavoidable uncertainty about parameters of the NS interfaces resulting from disorder near interface or appearance of oxide barrier that is typical for intermetallic junctions.

The original PtSi film with thickness of 6 nm was formed on Si substrate. The film had critical temperature  $T_c = 0.56$  K. The resistance per square was  $104 \Omega$ . The carrier density obtained from Hall measurements was  $7 \cdot 10^{22} \text{ cm}^{-3}$ , corresponding to the mean-free path  $l = 1.2$  nm and the diffusion constant  $D = 6 \text{ cm}^2/\text{s}$  estimated assuming the simple free-electron model. The initial samples used in the experiments were Hall bridges with  $50 \mu\text{m}$  in width and  $100 \mu\text{m}$  in length.

To fabricate 2D array we patterned the square lattice of holes covering the whole Hall bridge by means of electron lithography and subsequent plasma etching. The micrograph of the lattice are shown in Fig. 1c. The lattice constant is  $2.1 \mu\text{m}$  and diameter of holes  $1.7 \mu\text{m}$ , so the width of the narrowest part is  $0.4 \mu\text{m}$ . Thus we obtain the structure which consists of the islands of the film, with characteristic dimension being  $1.3 \mu\text{m}$ , connected by narrow necks. As the constrictions are not superconducting we have a two-dimensional array of SNS junctions (Fig. 1d). To do a comparative study, single SNS junctions were made with the same dimensions of constrictions, as shown in Fig. 1a,b.

The measurements were carried out with the use of a phase sensitive detection technique at a frequency of 10 Hz that allowed us to measure the differential resistance ( $R = dV/dI$ ) as a function of the dc voltage ( $V$ ). The ac current was equal to 10 nA. Figure 2 shows typical dependences of  $dV/dI$ - $V$  for the structures with a single SNS junction. The data exhibit a behavior very similar to that reported in the previous work [13]. The differ-

ential resistance reveals a minimum at zero bias voltage and reaches  $R_N \sim 530 \Omega$  at  $V_{ZBA} \sim 140 \mu\text{V}$  ( $R_N$  is the difference between the resistance of the whole structure with constriction and the resistance of the original film at  $T > T_c$ ). As one can see from the uppermost curves obtained at the highest temperatures, the zero bias anomaly survives even under the condition of fluctuation superconductivity and has the same voltage scale as that at the lowest temperatures.

In Fig. 3 we present the temperature dependence of the resistance for one of the two-dimensional arrays of SNS junctions. We have investigated three samples and found the similar behavior. At the temperatures higher than the superconducting transition temperature (this part of the curve is also shown in the lower inset to Fig. 3a) we observe the logarithmic behavior of the conductivity described by  $G(T) = G_{00} \ln(k_B T \tau / \hbar)$ , where  $G_{00} = e^2 / (2\pi^2 \hbar)$ . It indicates the effects of the weak localization and interaction in the diffusion channel in quasi-two-dimensions. As  $T_c$  is approached, the increase of the resistance slows down and at a temperature slightly lower than  $T_c$  it changes to quick decrease which proceeds down to the lowest temperature. The low-temperature part of the curve is presented in the top inset to Fig. 3a. This behavior can be considered as a transition from a 2D logarithmic weak localization to a metallic one due to the proximity effects. The transition region is depicted in Fig. 3b. It should be noted that the resistance of the original PtSi film nearby  $T_c$  is determined by the large contribution from the superconducting fluctuations. Here a deviation from the logarithmic behavior, originated from the superconducting fluctuations, becomes apparent at  $T \sim 0.8$  K. As it will be seen from the following results, the rapid decrease of the resistance observed at  $T \sim 0.45$  K, that is less than  $T_c$  of the unpatterned film, is not due to the superconducting transition in the islands. The latter occurs at a higher temperature. Thus the transition region is determined by an interplay of several different contributions: (a) the weak localization, (b) the superconducting fluctuations, and (c) the proximity effects.

The differential resistance measurements on the two-dimensional array of SNS junctions shown in Fig. 4 represent the key data of this Letter. The differential resistance has a minimum at zero bias voltage and shows a maximum at a finite bias voltage of about  $10 \mu\text{V}$  followed by a rapid decrease and eventually a slow decrease at large biases. In comparison with single SNS junctions where the zero-bias resistance dip extends to  $\sim 140 \mu\text{V}$  for 2DSNS we observe significant narrowing of the ZBA. It is less than  $10 \mu\text{V}$ . At nonzero biases a pronounced and fully symmetric structure in the differential resistance is seen. It is the so-called subharmonic energy gap structure (SGS) originated from the multiple Andreev reflections. In the general case the positions of these features are determined by the condition  $eV = \pm 2\Delta/n$ , with

( $n = 1, 2, 3, \dots$ ). As the right panel in Fig. 4b shows, the dips corresponding to  $n = 2, 4, 5, 6, 8, 10, 16$  manifest in our case. The presence of SGS in curves 2 and 3 indicates clearly that in this temperature region the islands are already superconducting. The precise shape of the structure which we observe for all 2D arrays of SNS junctions varies from sample to sample, with even  $n$  being commonly more pronounced and some  $n$  being absent. Summarizing the observations concerning to the appearance of SGS in our single and multiply connected SNS systems one can say that the structure reveals in both systems, with it being richer in 2DSNS. It should be noted that from the earlier theory [14] describing the subgap current transport in terms of ballistic propagation of quasiparticles it follows that there is no chance to observe the SGS in the case of the high-transparent NS interfaces. The SGS on current-voltage characteristics of single diffusive SNS junctions was observed in the works [10–13] and has only just been explained in a recent paper [15]. Following the spirit of Nazarov’s circuit theory [16], authors of Ref. [15] show that unlike the ballistic case in long diffusive SNS junctions the SGS survives even for perfect NS interfaces. It occurs owing to coherent impurity scattering of the quasiparticles inside the proximity region that formally corresponds to renormalized value of the interface resistance.

The issue to be addressed now is the behavior of the differential resistance at zero bias. For all samples under study we observe the dip, with the value of  $\Delta R_{\text{SNS}}/R_N$  being more than 10%. It is the so-called excess conductance experimentally observed in all single diffusive SNS junctions [5–13]. ZBA observed in our single SNS junctions is likely to be the result of interplay of non-local coherent effects, namely (i) the superposition of multiple coherent scattering at the NS interfaces in the presence of disorder (so-called reflectionless tunneling [17]) and (ii) the electron-electron interaction in the normal part. The latter is one of the important points of recently developed “circuit theory” when applied to diffusive superconducting hybrid systems [18]. Within this approach, which is based on the use of the nonequilibrium Green function method, the electron-electron interaction induces weak pair potential in the normal metal. It results not only in the change of the resistance, but in a non-trivial distribution of the electrostatic and chemical potentials in the structure as well, that implies non-local resistivity in the structure. It is essentially a consequence of coherent nature of Andreev reflection. The most striking feature is, as the results for 2D array of SNS junctions presented in this Letter show, that self-averaging is totally absent and coherence of the effects governed by Andreev reflection is maintained over the entire sample. Moreover, in comparison with single SNS junction the manifestation of the effects in 2DSNS systems (particularly the SGS) is far more pronounced. The behavior of the ZBA and SGS in 2D array of SNS junctions strongly suggests that

the development of a novel theoretical approach is needed which would self-consistently take into account the distribution of the currents, the potentials, and the superconducting order parameter. In this connection a recent work [19] should be noted, where the authors have extended the theoretical approach to disordered systems based on the nonlinear  $\sigma$ -model. An advantage of this approach is, unlike the others where the superconducting order parameter was taken into account just by the boundary conditions for the normal region, that it makes possible to describe an effect on the superconducting order parameter of disorder in the normal metal and even inside the superconducting region. As a consequence it was shown that the size of the superconductor influences the proximity effects. In our case this can be a probable reason for a drastic decrease of the effective suppression voltage for the ZBA when we turn from a single SNS system to multiply connected SNS junctions.

In summary, we have performed the first comparative study of two-dimensional array of diffusive SNS junctions and single SNS junction. Our experiments show that coherent phenomena governed by the Andreev reflection are not only maintained over the macroscopic scale but manifest novel pronounced effects as well. To have clear physical understanding of the phenomena observed in mesoscopic multiply connected systems further theoretical progress is needed.

We thank R. Donaton and M. Baklanov (IMEC) for providing the PtSi films. We would like to acknowledge valuable conversation with M. Feigel'man and Yu. Nazarov. This work has been supported by the program "Physics of quantum and wave processes" of the Russian Ministry of Science and Technology and by RFBR Grant No. 00-02-17965.

- Phys. Rev. Lett. **76**, 130 (1996); P. Charlat, H. Courtois, Ph. Gandit, D. Mailly, A. F. Volkov and B. Pannetier, *ibid.* **77**, 4950 (1996).
- [9] X. Jehl, P. Payet-Burin, C. Baraduc, R. Calemczuk, and M. Sanquer, Phys. Rev. Lett. **83**, 1660 (1999).
- [10] J. Kutchinsky, R. Taborski, T. Clausen, C. B. Sørensen, A. Kristensen, P. E. Lindelof, J. Bindslev Hansen, C. S. Jacobsen, and J. L. Skov, Phys. Rev. Lett. **78**, 931 (1997).
- [11] A. Frydman and R. C. Dynes, Phys. Rev. B **59**, 8432 (1999).
- [12] T. Hoss, C. Strunk, T. Nussbaumer, R. Huber, U. Staufer, and C. Schonenberger, Phys. Rev. B **62**, 4079, (2000).
- [13] Z. D. Kvon, T. I. Baturina, R. A. Donaton, M. R. Baklanov, K. Maex, E. B. Olshanetsky, A. E. Plotnikov, and J. C. Portal, Phys. Rev. B **61**, 11340 (2000).
- [14] M. Octavio, M. Tinkham, G. E. Blonder, and T. M. Klapwijk, Phys. Rev. B **27**, 6739 (1983); K. Flensberg, J. Bindslev Hansen, M. Octavio, *ibid.* **38**, 8707 (1988).
- [15] E. V. Bezuglyi, E. N. Bratus', V. S. Shumeiko, G. Wendin, and H. Takayanagi, cond-mat/0005387.
- [16] Yu. V. Nazarov, Phys. Rev. Lett. **73**, 1420 (1994); Superlattices Microstruct. **25**, 1221 (1999).
- [17] B. J. van Wees, P. de Vries, P. Magnee, and T. M. Klapwijk, Phys. Rev. Lett. **69**, 510 (1992); C. W. J. Beenakker, Phys. Rev. B **46**, 12841 (1992); I. K. Marmoros, C. W. J. Beenakker, R. A. Jalabert, *ibid.* **48**, 2811 (1993).
- [18] Yu. V. Nazarov, and T. H. Stoof, Phys. Rev. Lett. **76**, 823 (1996); T. H. Stoof, and Yu. V. Nazarov, Phys. Rev. B **53**, 14496 (1996).
- [19] I. V. Yurkevich, I. V. Lerner, cond-mat/0006378.

- 
- [1] B. Pannetier and H. Courtois, J. of Low Temp. Phys. **118**, 599 (2000).
- [2] A. Kastalsky, A. W. Kleinsasser, L. H. Greene, R. Bhat, F. P. Milliken, and J. P. Harbison, Phys. Rev. Lett. **67**, 3026 (1991).
- [3] C. Nguyen, H. Kroemer, and E. Hu, Phys. Rev. Lett. **69**, 2847 (1992).
- [4] W. M. van Hufelen, T. M. Klapwijk, D. R. Heslinga, M. J. de Boer, and N. van der Post, Phys. Rev. B **47**, 5170 (1993).
- [5] P. Xiong, G. Xiao, and R. B. Laibowitz, Phys. Rev. Lett. **71**, 1907 (1993).
- [6] V. N. Petrashov, V. N. Antonov, P. Delsing, and R. Claesson, Phys. Rev. Lett. **70**, 347 (1993).
- [7] P. H. C. Magnee, N. van der Post, P. H. M. Kostra, B. J. van Wees, and T. M. Klapwijk, Phys. Rev. B **50**, 4594, (1994).
- [8] H. Courtois, Ph. Gandit, D. Mailly, and B. Pannetier,

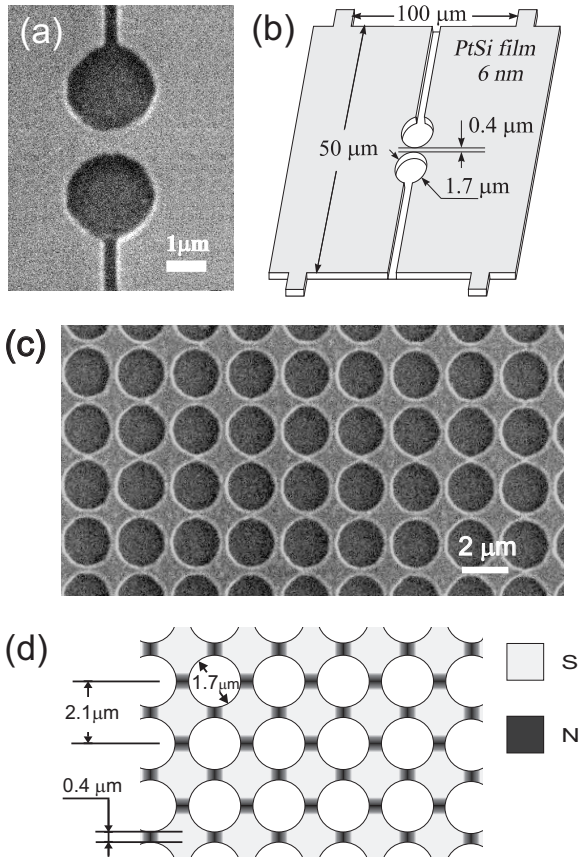


FIG. 1. (a) Scanning electron micrograph of the sample with single constriction formed by electron beam lithography and subsequent plasma etching of the 6 nm PtSi film grown on Si substrate. (b) Schematic view of a junction (not to scale) showing the layout of the constriction in the Hall bridge. (c) SEM subimage of square lattice of holes made in PtSi film. (d) The layout of a two-dimensional array of SNS junctions showing the dimensions of the sample. Regions of the normal metal constrictions are dark, and the superconducting islands are light gray.

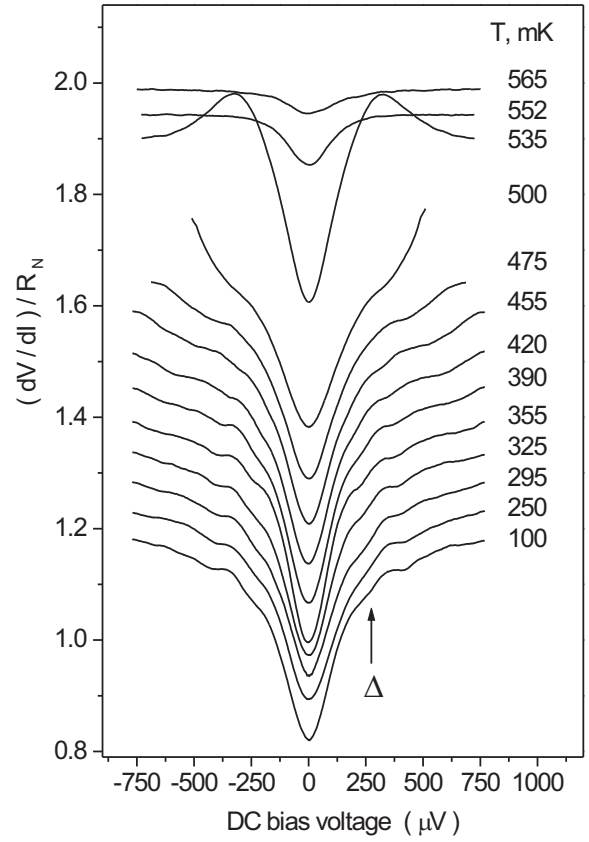


FIG. 2. Normalized differential resistance  $(dV/dI)/R_N$  of a single SNS junction as a function of bias voltage at different temperatures. (All traces except the lowest trace are successively shifted upward by 0.05, for clarity.) The subharmonic energy gap structure is smeared and can be seen more clearly on the dependence of  $d^2V/dI^2-V$ . The arrow indicates  $eV = \Delta$  corresponding to the maximum slope.

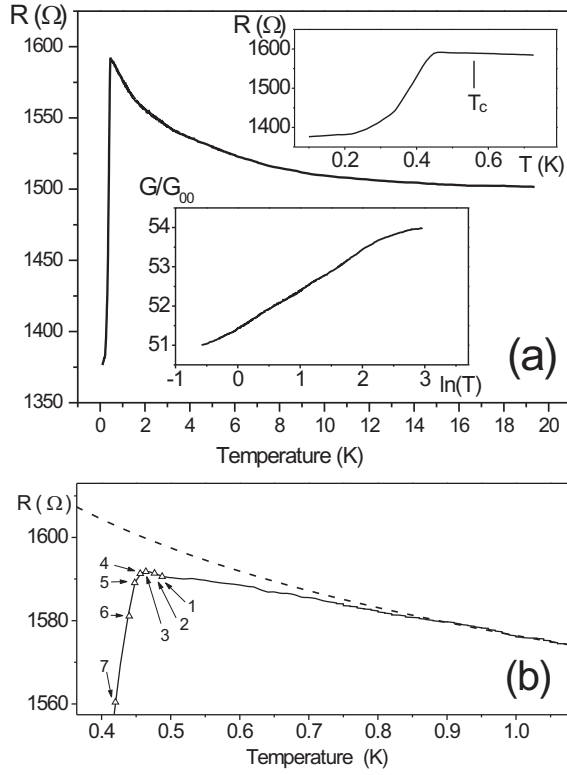


FIG. 3. (a) Temperature dependence of the resistance per square for a two-dimensional array of SNS junctions. The top inset represents the low-temperature part of the dependence. The bottom inset shows the conductance in units of  $G_{00} = e^2/(2\pi^2\hbar)$  vs  $\ln(T)$  at  $T > T_c$ . (b) The solid curve represents the temperature dependence of the resistance nearby  $T_c$ . The dashed line is the fit to  $1/R(T) \propto \ln(T)$ . The numbered triangles are zero-bias resistance extracted from the  $dV/dI-V$  presented in Fig. 4b (left panel).

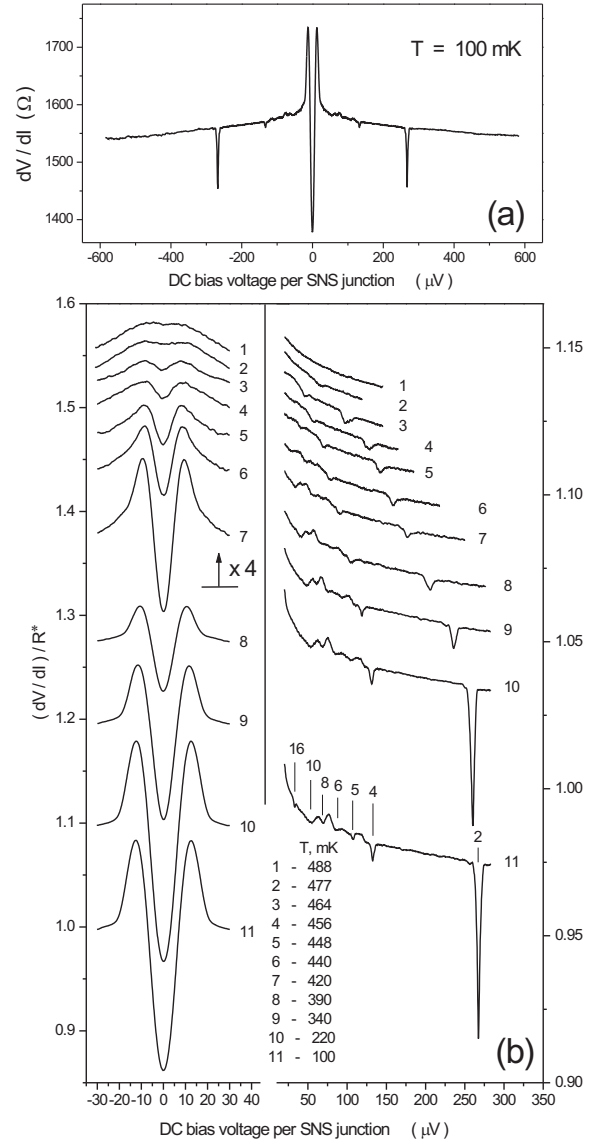


FIG. 4. (a) Differential resistance of the sample with a two-dimensional array of SNS junctions as a function of the bias voltage falling at one SNS junction at  $T = 100$  mK showing a sharp zero-bias resistance dip followed by above-normal peak. The differential resistance possesses the subharmonic energy gap structure that is seen as symmetrical minima in a range of voltages from  $\sim 30 \mu\text{V}$  to  $\sim 300 \mu\text{V}$ . (b) Temperature evolution of the normalized differential resistance ( $R^* = 1600 \Omega$ ) vs dc bias voltage divided by the number of SNS junctions between the measuring probes. (All traces except the lowest trace are shifted up for clarity.) The left panel shows a low-voltage part of the curves. (Note the change of height scale in the upper 7 traces.) The traces in the right panel are continuations of the ones presented in the left panel to higher voltage. The curves are numbered according to the temperatures listed at the bottom.